

# The performance of the calibration module for SPHERE

Francois Wildi<sup>1</sup>, Bernard Michaud<sup>1</sup>, Michel Crausaz<sup>1</sup>, René Dubosson<sup>1</sup>, David Mouillet<sup>2</sup>, Kjetil Dohlen<sup>3</sup>, Hans-Martin Schmid<sup>4</sup>, Jean-Luc Beuzit<sup>2</sup>

<sup>1</sup> Observatoire de Genève, CH-1290 Sauverny, Switzerland

<sup>2</sup> Laboratoire d'Astrophysique de Grenoble, B.P. 53, F-38041 Grenoble Cedex 9, France

<sup>3</sup> Laboratoire d'Astrophysique de Marseille, B.P. 8, F-13376 Marseille Cedex 12, France

<sup>4</sup> Institute of Astronomy, ETH Zurich, CH-8092 Zurich, Switzerland

## ABSTRACT

One of the main challenges to obtain the contrast of  $>15$ mag targeted by the extra-solar planet imager SPHERE lies in the calibration of all the different elements participating in the final performance. The Adaptive Optics (AO) system and its three embedded loops, the coronagraphs, the Near Infrared (NIR) dual band imager, the NIR integral field spectrograph, the NIR spectrograph, the visible high accuracy polarimeter and the visible imager all require sophisticated calibration. The calibration process relies on a specific complex calibration module that provides the different sources across the spectrum (500-2320nm) with the stabilities and precisions required and positions them when the need to be. This calibration module has just passed all verification tests and its performance is now well characterized. Its design and performance is the object of this article.

**Keywords:** exo-solar planets, extreme adaptive optics, coronagraphy, dual band imaging, polarimetry, spectral imaging

## 1. INTRODUCTION

The prime objective of the Spectro-Polarimetric High-contrast Exoplanet Research (SPHERE) instrument for the VLT is the discovery and study of new extra-solar giant planets orbiting nearby stars by direct imaging of their circumstellar environment. The challenge consists in the very large contrast between the host star and the planet, larger than 12.5 magnitudes (or  $10^5$  in flux ratio), at very small angular separations, typically inside the seeing halo. The design of SPHERE is optimized towards reaching the highest contrast in a limited field of view and at short distances from the central star. The design of SPHERE and its expected performance has been the subject of prior publications [1], [2] and [3].

Calibration is of paramount importance to reach the expected high contrast of the instrument: The static transfer functions of the extreme adaptive optics system must be measured to optimize the close loop performance, the non-common path aberrations need to be measured to maximize the coronagraph performance and more classically the detectors response must be characterized. In general a maximal number of instrumental effects are measured to minimize their influence on the final performance. The number of calibration modes of SPHERE is almost tenfold larger than the operation modes.

## 2. THE SPHERE INSTRUMENT

SPHERE is divided into four subsystems: the Common Path and Infrastructure (CPI) and the three science channels: a differential imaging camera (IRDIS, InfraRed Dual Imaging Spectrograph), an Integral Field Spectrograph (IFS) and a visible imaging polarimeter (ZIMPOL, Zurich Imaging Polarimeter). The Common Path includes pupil stabilizing fore optics (tip-tilt and rotation), calibration units, the SAXO extreme adaptive optics system, and NIR and visible coronagraphic devices. IRDIS provides wide-field imaging in one or two

---

<sup>1</sup> francois.wildi@unige.ch

simultaneous spectral bands or two orthogonal polarizations and low and medium resolution long slit spectroscopy. The IFS, working from 0.95 to 1.65  $\mu\text{m}$ , provides low spectral resolution ( $R \sim 30$ ) over a limited, 1.8" x 1.8", field-of-view. A photon sharing scheme has been agreed between IRDIS and IFS, allowing IFS to exploit the NIR range up to the J band, leaving the Hband, judged optimal for the DBI mode, for IRDIS for the main observation mode. ZIMPOL is a high precision polarimeter covering 600 to 900 nm. It achieves a polarimetric precision of  $10^{-5}$  or better by a modulation scheme that allows the simultaneous detection of two perpendicular polarizations (the modulation is faster than seeing variations), and the recording of both images on the same pixel. The CCD covers a Nyquist sampled field of 3" x 3". In addition to polarimetric imaging, ZIMPOL provides the possibility for high-resolution imaging in the visual range using a set of broad and narrow-band filters. The current implementation of SPHERE at the Nasmyth focus of the VLT is shown in Fig. 1 (R/h).

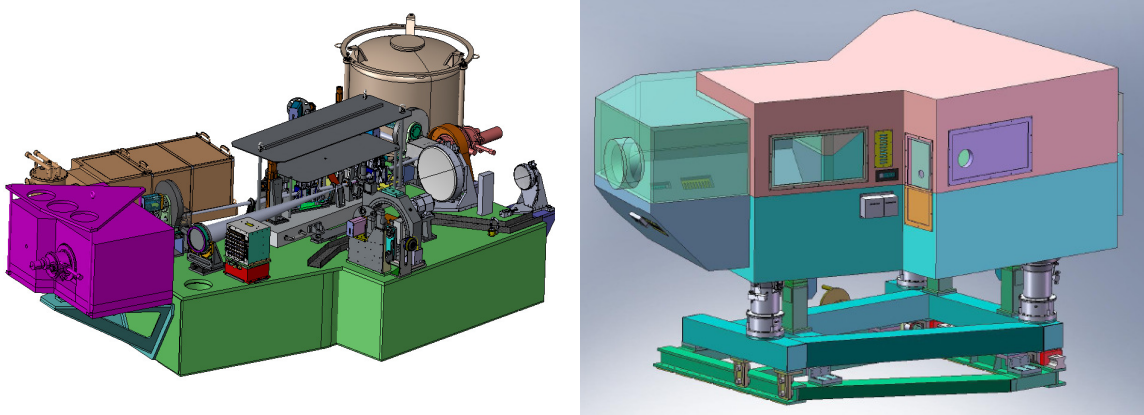


Fig. 1. The view on the left shows the complete SPHERE opto-mechanical assembly. The view on the right shows how SPHERE will look like in operation, when the opto-mechanical assembly is mounted onto the vibration damping system and into the thermal-vacuum enclosure.

### 3. CALIBRATION REQUIREMENTS AND PERFORMANCE

#### 3.1 Detectors

SPHERE uses 2 H2RG infrared science detectors one for IRDIS and one for the IFS [5] and [7], 2 visible science detector (both for ZIMPOL, [8]), one visible and one infrared wavefront sensing detectors. All these detectors need classical dark fielding, and flat fielding.

Due to the specificity of the high contrast capability required for the imaging of extra-solar planets, the most critical performance of the calibration module is the homogeneity of the flat field, especially a small scale. The most stringent requirement coming from the DBI is 99.9% homogeneity from pixel to pixel and 99.9% homogeneity within a 10x10 pixel area. In addition, to make precise measurement possible the flat field source must also be bright to beat the photon noise.

We have opted for an integrating sphere to implement this source. To the 1<sup>st</sup> order the radiance of an integrating sphere is proportional to the inverse of the diameter, calling for a small sphere. On the other hand a larger sphere will better average the local non-uniformities of the sphere as suggested on fig 2. A trade study led us to choose the largest possible sphere to minimize the non-uniformity and the source chosen is an incandescent lamp which, of course, because of the thermal constraints, cannot be located inside the sphere. The light guide and the feed system were designed to guarantee sufficient flux.

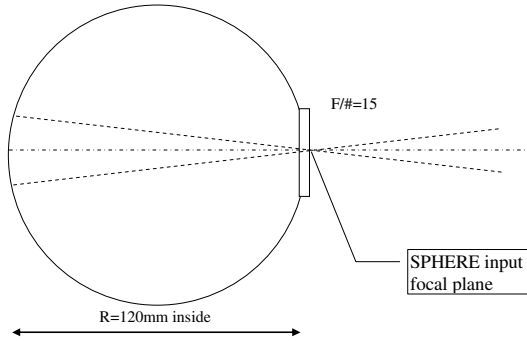


Fig 2: A large integrating sphere helps defocusing the internal side of the sphere as seen by the instrument and homogenizes the flat field at high spatial frequencies. If the diameter is large, the footprint of the beam at the back of the sphere is mostly the same for 2 adjacent pixels.

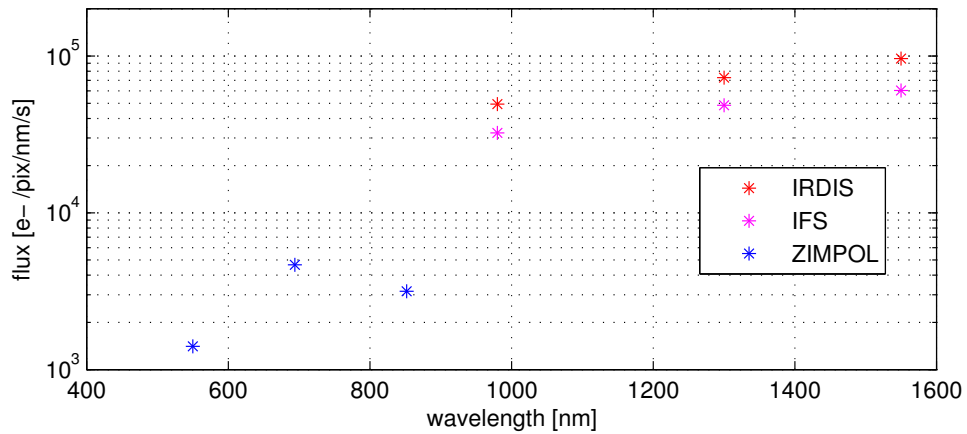


Fig 3: The measured spectral flux per pixel from the flat field calibration source expected at the detector level (including SPHERE transmission and detector QE). The nature of the source limits the flux available in the visible. During integration, it is planned to overdrive the QTH bulbs at the cost of lifetime to look for the ZIMPOL detectivity limits

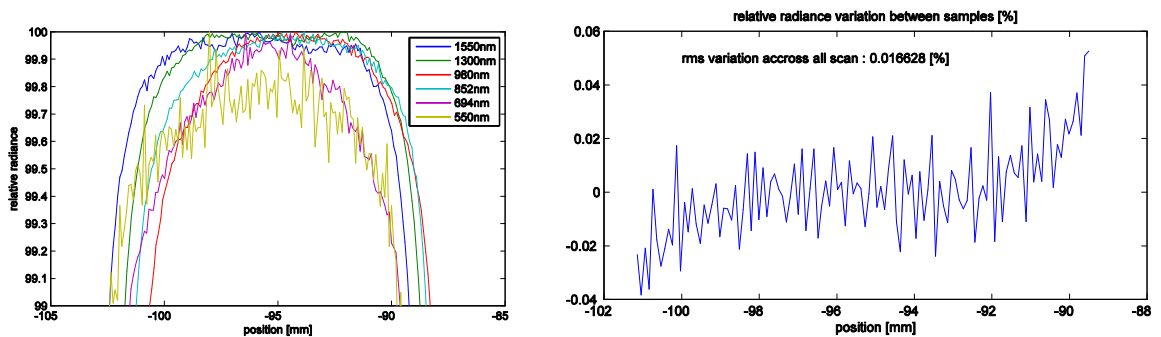


Fig 4: The flat field uniformity on the large scale is very satisfactory, being better than 0.5% center to edge. When averaging to have high enough SNR, the mid scale uniformity is  $10^{-4}$  rms and the pixel scale uniformity is  $10^{-3}$  (SNR limited).

### 3.2 Adaptive optics

The adaptive optics loops require a significant number of calibrations: Wavefront sensor zero, and interaction matrices (the measurement of the relationship between actuator activation and sensor measurement) have to be measured between various active optics and sensors.

All in all AO requires a significant number of calibrations, but they do not put strong constraints on the calibration hardware: Point sources of sufficient flux will do the job. With 1350 sub-apertures, read at 1200 fps, each requiring 1000 detected photo-electrons; this does indeed mean  $10^{10}$  ph/s entering the system.

### 3.3 Static and quasi-static aberrations correction

The performance in high contrast imagery depends very much on the ability of the AO to reach the highest correction on the coronagraphic focal mask. There are 2 parts in the correction error: a dynamic part due to the atmospheric turbulence and a static part due to the presence of static aberrations in the corrected wavefront. These static aberrations can be greatly reduced by calibration which leads to a significant reduction of the static speckles (see [9]). To correct the static aberrations, we are measuring then using phase diversity. By measuring the static aberrations between the input focus and the science detector and the aberrations between the coronagraphic focus and the science detector, we are able to infer the aberrations between input focus and coronagraphic focus [4]. This calibration requires diffraction limited sources covering the science channels spectra with sufficient throughput for high SNR imaging of defocused images.

It also requires two sources on the optical axis located in the vicinity of the coronagraphic focal planes, which separation is precisely known. In our implementation, we are using a single fiber source mounted on a precision lead screw type motion stages. Qualification of all these stages on an interferometer have shown that providing we allow for an hysteresis term in the motion equation, the positioning error can be brought down to about  $1\mu\text{m}$  rms (see below) but that an error term at the spatial frequency of the lead screw pitch must be introduced to get further down. However, the repeatability between 2 positions is always smaller than  $1\mu\text{m}$  p2v, 50% of our budget

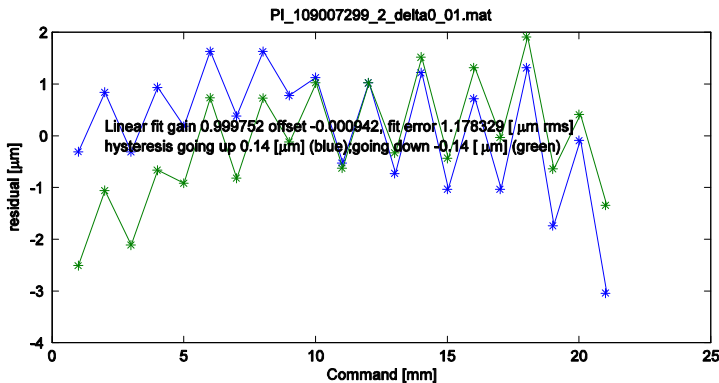


Fig 5: Characterization of each precision motorized stage used for phase diversity measurements was performed with an interferometer (R/h). After hysteresis correction the error curve shows a significant residual at a frequency of  $0.5/\text{mm}$ , a sub-harmonic of the pitch of the lead screw of  $2/\text{mm}$  that would prevent reaching the required accuracy. The stages were finally characterized between 2 fixed positions, with sub-micrometer repeatability.

### 3.4 Coronagraphs

For the proper simulation of the effect of the coronagraph, the homogeneity of the pupil illumination is an important parameter. After simulation, the homogeneity requirement was set at 10% center to edge versus 0% on a real star. A numerical model of the monomode fibers used predicted that the homogeneity would exceed specification based on the numerical aperture (N.A.) given by the manufacturer. In practice, this holds true for the longest wavelength, but not in the shorter part of the range as shown on figure 6 below. Since there is little freedom in the choice of the fibers N.A. we had to agree to take the effect of the non-homogeneity into account when

processing the calibration data, rather than investing significant resources in retro-fitting re-imaging optics in the point sources hardware.

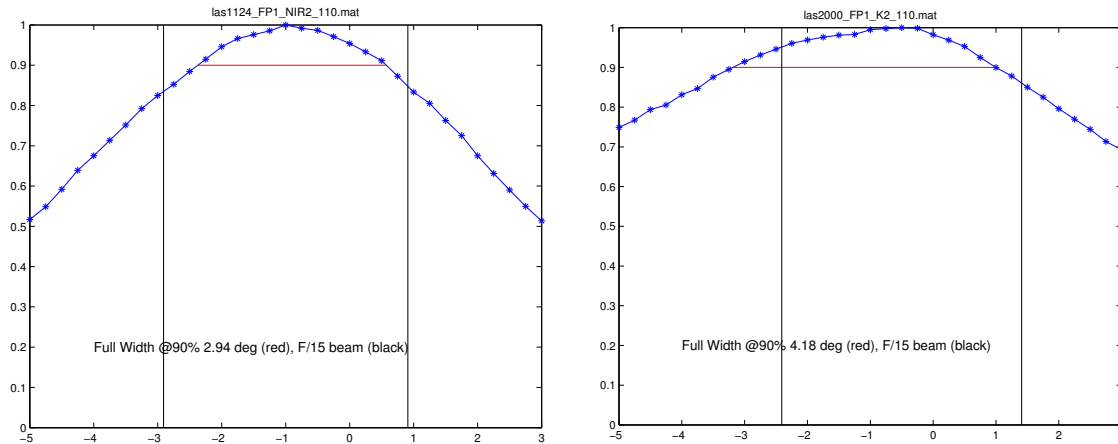


Fig 6: Far field density of the point sources. The vertical lines represent the edges of the F/15 beam entering SPHERE. Ideally, the artificial stars of the calibration system would mimic the real ones seen through the VLT; featuring homogenous pupil illumination. On the short side of the range this is not the case with over 10% variation center to edge (L/h) while at longer wavelength the situation is more satisfactory (R/h).

### 3.5 Imaging

The calibration of the imaging mode also requires that a wide spectrum source is available for the characterization of the field distortion. To this purpose a motorized stage can slide of Zerodur grating in front of the flat filed source.

The calibration of SPHERE also requires that point sources are available for the characterization of the ghosts and to test the quality of the AO loop. Their size must be  $< \lambda/2D$ , to be unresolved on the detector. These sources are made of monomode optical fibers. To optimize to flux and the homogeneity, 3 different fibers cover the wavelength range, with a special fluoride fiber covering the K-band.

To be able to run the AO system at full speed, the broadband source is supplemented with a visible laser, so that the flux is sufficient. Depending on the fiber, the laser beam will not be monomode, but this will not impact the wavefront sensor which resolution is  $\lambda/d$ , where  $d$  is the diameter of a subaperture.  $d = D/40$ .

### 3.6 Spectroscopy

Another hard point was the production of a spectral source with full coverage adequate for the modest resolution for the Integral Field Spectrograph, and still stable enough for the Medium Resolution Spectroscopy mode of IRDIS [6](stability of 0.05nm over the instrument lifetime is required). Traditional spectral lamps have a much too dense set of lines that cannot be resolved by the low resolution spectroscopy. The gap required for a Fabry-Perot etalon would correspond to a few waves (i.e  $< 10$  micron) which is both too thin to guarantee a manufacturable air-spaced etalon and too thick for a thin film deposited one. We have opted for fiber-fed temperature stabilized distributed fiber Bragg grating laser diode (DFB). With a typical linewidth  $< 0.01$ nm these lasers are much below the resolution limit of the spectroscopic modes, allowing characterization of the Line Spread Function (LSF) of the slit spectroscopy mode. Based on experience we were expecting a stability of these devices of about 10 GHz, or 0.03 nm @ 1000nm, when properly temperature and power controlled is. Measurements have confirmed that our set-up is largely immune from the ambient temperature variations at the telescope, featuring stability of 30pm rms or better during the temperature tests.

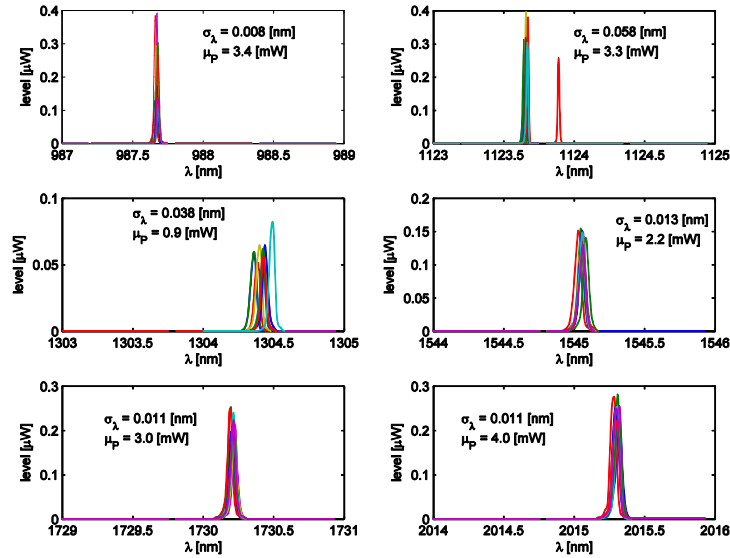


Fig 7: Spectrum of each laser line during the multi-cycle temperature test. . The variation is about 0.01nm for most lines, and in all cases <0.03nm

Both the IFS and IRDIS perform field spectroscopy (although IRDIS samples only along its slit). Therefore, the spectral sources need to cover the full field of view (FOV). This is why our DBG laser diodes are fiber coupled to the integrating sphere.

To determine the LSF of IRDIS in spectroscopic mode, part of the light of 2 spectral lines is coupled to a single mode fiber forming a source unresolved spatially and spectrally.

### 3.7 Polarimetry

The calibration of the polarimetric mode requires therefore: (a) the possibility to disentangle a very weak point-like polarization flux signal which is  $10^5$  times weaker than the PSF intensity from any spurious (instrumental or atmospheric) polarization features, (b) the possibility to measure extended polarization signals, e.g. scattered light from disk, with a polarization flux which is  $10^3$  times less than the PSF intensity (c) a determination of the zero point of the polarization position angle with a precision of a 1 to 3 degrees, (d) knowledge of the polarimetric efficiency with a precision of a few %.

The requirements (a) and (b) are very demanding and besides a good calibration they require as prerequisite a very sophisticated polarimetric measuring strategy. The ZIMPOL polarimeter (single beam - fast modulation / demodulation) is a measuring principle which is in a certain sense "self-calibrating". For example no (intensity) flat-field calibrations are required thanks to the special differential measuring technique employed.

ZIMPOL measures the polarization at the position of the fast modulator. The measured polarization is therefore composed of the polarization from the target (sky) and all the polarization effects introduced by the optical components in front of the polarization modulator. Thus the measurements must be calibrated for all the polarization effects introduced by the telescope and inside the instrument. This is done with insertable calibration components (linear polarizer, quarter wave retarder plate, and circular polarizer) in the common path and in ZIMPOL itself. These components are not part of the SPHERE calibration module and their performance is not addressed in this article.

## 4. CALIBRATION HARDWARE DESIGN

The design of the calibration unit was constrained by the fact that the temperature of SPHERE is uncontrolled and can vary between 0C and 15C. In addition, inside the SPHERE thermal enclosure, the temperature of any

component cannot be different by more than 0.4C from the ambient for internal turbulence reasons. Furthermore, the telescope chamber is inaccessible during the night and all operations have to be remote controlled.

#### 4.1 Concept

The calibration unit is built in two parts: a source unit is hosting the sources proper and the control rack. On the other side, a feed unit delivers the light from the sources inside SPHERE. The source unit features infrared lasers, a Quartz Tungsten Halogen (QTH) lamp with two incandescent bulbs in cold redundancy, conditioning optics, a filter wheel and a linear stage where different fibers can be fed by the lamp.

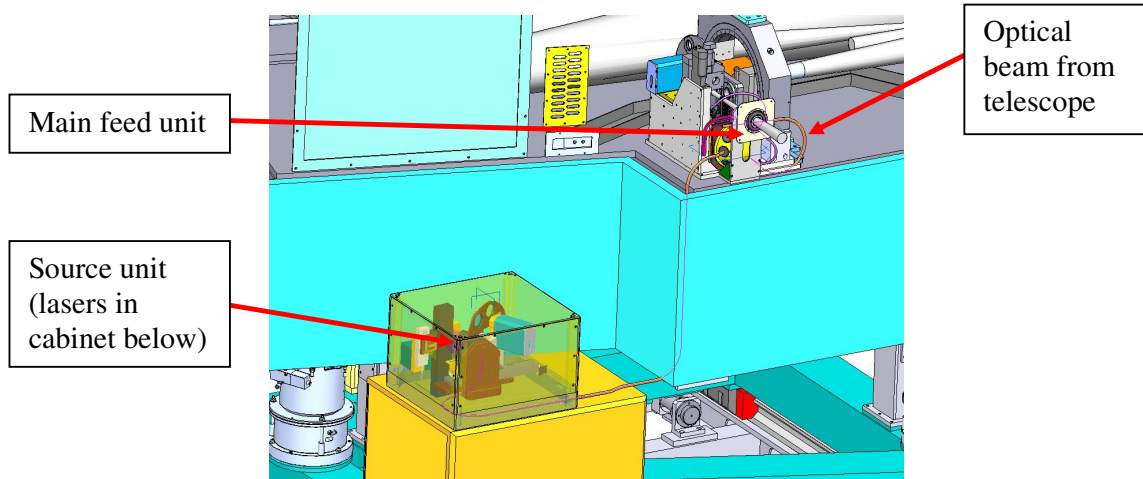


Fig 8: 3D view of the calibration unit installed on SPHERE. The source unit sits outside the thermal/dust enclosure for thermal reasons. The main feed unit is located at the VLT Nasmyth focus

#### 4.2 Implementation

A single lamp with an incandescent lamp is used for all sources but the spectral ones. It is equipped with a source selector stage, a bulb exchange stage (for redundancy) and a neutral density filter wheel. Inside SPHERE, the main feed unit features 3 broad band point sources, a spectral point source to measure the spectrographs LSF, the flat filed source and the distortion calibration mask. A linear stage allows refocusing when polarization components are introduced in the optical train, which moves the input focus point towards the telescope.

The spectral sources are separate from the broadband source and separate from each other. On one side they feed the flat field integrating sphere where they mix into the sphere, providing a spectral flat field that is vital for the wavelength calibration of the IFS. On the other side, a small part of flux of 2 spectral lines is coupled and injected in a monomode fiber to form a spectral point source that we use to characterize the point spread function of IRDIS in slit spectroscopy mode

#### 4.3 Operations

The calibration module is a complex element, critical to allow SPHERE to reach its nominal performance. In addition, because of light throughput issues, it is located in a hard to reach location between the VLT nasmyth rotator and the SPHERE thermal enclosure. There considerations have lead us to think very early at operational issues like reliability, diagnostic and maintainability.

Flat fielding requirements for SPHERE are really tight, in particular for the integral field spectroscopy where flat filed exposures must be taken in-between science exposures, when the telescope is repointing. A night without flat fielding capability is essentially lost. This is why a fully redundant flat field lamp is provided (bulb and bulb power supply). The spare bulb can be put in place and the space power tuned on remotely at any time via the control system. During day-time operations, a pre-aligned 2-bulb module can be exchanged in a minimal amount of time. Two-stage ventilation inside the lamp reduces the stress on the bulb and removes the heat to keep the enclosure below ambient.

Essentially all remote commands to the calibration unit can be monitored with a corresponding telemetry: The optical power of the calibration system can be monitored with photodiodes looking at the lamp and at the flat field so that both the absolute power and the transmission of the light guide can be assessed. Temperatures at different point in the lamp allow fan failures to be diagnosed.

Temperature and current monitoring in the spectral sources allow remote diagnostic of the electronic drivers; the monitoring of the lasers optical power being performed with the flat field photodiodes.



Fig 9: Photographs of the source unit (L/h) and the main feed unit (R/h) of the calibration module. The point sources on the feed unit are mounted on an horizontal stage (Z-axis) to allow re-focusing when the polarization components are inserted in the beam, which changes the location of the SPHERE input object point. X and Y motions allow for precise centering on the coronagraphs. The SPHERE field stop can be seen above the fiber point sources. Once fully integrated, this assembly is almost hidden behind the rotating half-wave plates of the polarization mode.

## 5. CONCLUSION

The performance of a high contrast imager like SPHERE depends crucially on the calibration of the different instrumental artifacts. In our case the complexity of the calibration is significant and required a significant effort in terms of definition, requirements collection and design. The calibration of SPHERE involves 12 motors, 9 different light sources, an extensive control system and it makes up 90 instrument modes while the operation modes total only 11.

The SPHERE calibration module development was complete in the middle of 2009. Its manufacturing phase lasted throughout 2009 with integration in the last quarter. Tests were performed in the first 5 months of 2010.

This module is now fully characterized and verified. It has passed Acceptance Readiness Review in June 2010 and is now undergoing the last few modifications before shipment to the SPHERE integration facility.

It complies with the vast majority of its applicable specifications; and where not, the non-compliances are accepted. We are looking for an exciting when it is used to characterize SPHERE and when SPHERE data can be used to further characterize this module



## REFERENCES

- [1] J.-L. Beuzit, M. Feldt, K. Dohlen, D. Mouillet, P. Puget, François P. Wildi, M. Kasper, and the SPHERE Consortium, "SPHERE: a planet imager for the VLT", in *Ground-based and Airborne Instrumentation for Astronomy III*, SPIE 7735-33 (2010)
- [2] F. Wildi, J.-L. Beuzit, M. Feldt, D. Mouillet, K. Dohlen, P. Puget, A. Baruffolo, J. Charton, P. Baudoz, A. Boccaletti, L. Abe, R. Claudi, Ph. Feautrier, T. Fusco, R. Gratton, N. Hubin, M. Kasper, M. Langlois, R. Lenzen, A. Pavlov, C. Petit, J. Pragt, P. Rabou, R. Roelfsema, M. Saisse, H.-M. Schmid, E. Stadler, M. Turatto, S. Udry, R. Waters, T. Henning, A.-M. Lagrange, F. Vakili. "SPHERE: The VLT exo-planet imager in the post-FDR phase", *Techniques and Instrumentation for Detection of Exoplanets IV*, SPIE 7440-24 (2009)
- [3] F. Wildi, D. Mouillet, J.-L. Beuzit, M. Feldt, K. Dohlen, T. Fusco, C. Petit, S. Desidera, R. Gratton, M. Langlois, H.-M. Schmid, A. Vigan, J. Charton, R. Claudi, R. Roelfsema, A. Baruffolo, P. Puget. "Calibrating SPHERE, the VLT extra-solar planet imager", in *Techniques and Instrumentation for Detection of Exoplanets IV*, SPIE 7440-25 (2009)
- [4] C. Petit, T. Fusco, J.-M. Conan, J.-F. Sauvage, G. Rousset., P. Gigan, J. Charton, D. Mouillet, P. Rabou, M. Kasper, E. Fedrigo, N. Hubin, Ph. Feautrier, J.-L. Beuzit, P. Puget, "The SPHERE XAO system: design and performance", in *Adaptive Optics Systems*, SPIE 7015-65 (2008)
- [5] K. Dohlen, M. Saisse, M. Langlois, M. Jaquet, A. Origine, A. Vigan., G. Arthaud, J.-L. Lizon, R. Dorn, G. Finger, R. Dorn, J.L. Beuzit, P. Puget, D. Mouillet, M. Feldt, F. Wildi, A. Baruffolo, M. Kasper, N. Hubin. "Manufacturing and integration of the IRDIS dual imaging camera and spectrograph for SPHERE" in *Ground-based and Airborne Instrumentation for Astronomy III*, SPIE 7735-154 (2010)
- [6] A. Vigan and M. Langlois and C. Moutou and K. Dohlen, "Long slit spectroscopy for exoplanet characterization in SPHERE", *Ground-based and Airborne Instrumentation for Astronomy II*, SPIE, 7014-
- [7] S. Desidera, R. Gratton, R. Claudi, J. Antichi, D. Mesa, M. Turatto,; P. Bruno, E. Cascone,; V. De Caprio, E. Giro; S. Scuderi; M. Feldt, A. Pavlov, K. Dohlen, J.-L. Beuzit, D. Mouillet, P. Puget, F. Wildi, "Calibration and data reduction for planet detection with SPHERE-IFS", in *Ground-based and Airborne Instrumentation for Astronomy II*, SPIE 7014-127 (2008)
- [8] R. Roelfsema, H.-M. Schmid, J. Pragt, D. Gisler, R. Waters, A. Bazzon, A. Baruffolo, J.-L. Beuzit, A. Boccaletti, J. Charton, C. Cumanif, K. Dohlen, M. Downing, E. Elswijk, M. Feld, Ch. Groothuis, M. de Haan, H. Hanenburg, N. Hubin, F. Joos, M. Kasper, Ch. Keller, J. Kragt, J.-L. Lizon, D. Mouillet, A. Pavlov, F. Rigal, S. Rochat, B. Salasnich, P. Steiner, Ch. Thalmann, L. Venema, F. Wildi. "The ZIMPOL high contrast imaging polarimeter for SPHERE: design, manufacturing and testing", in *Ground-based and Airborne Instrumentation for Astronomy III*, SPIE 7735-154 (2010)
- [9] J.-F. Sauvage, T. Fusco, G. Rousset, and C. Petit, "Real-time and post-facto correction for differential aberrations in direct planet imaging by adaptive optics," in IAUC 200, Direct Imaging of Exoplanets: Science & Techniques, 2005. Date conference : Oct. 2005, Nice, France.